

- <sup>16</sup>S. N. Lee, Ph. D. thesis (Iowa State University, 1968) (unpublished).
- <sup>17</sup>F. R. Kroeger and W. A. Rhinehart, *Rev. Sci. Instr.* **42**, 1532 (1971).
- <sup>18</sup>H. Fritzsche, *Phys. Rev.* **99**, 406 (1955).
- <sup>19</sup>A. Miller and E. Abrahams, *Phys. Rev.* **120**, 745 (1960).
- <sup>20</sup>N. F. Mott and W. D. Twose, *Advan. Phys.* **10**, 107 (1961).
- <sup>21</sup>H. Nishimura, *Phys. Rev.* **138**, A815 (1965).
- <sup>22</sup>E. A. Davis and W. D. Compton, *Phys. Rev.* **140**, A2183 (1965).
- <sup>23</sup>H. Brooks, in *Advances in Electronics and Electron Physics*, Vol. VII, edited by L. Marton (Academic, New York, 1955), pp. 102–104.
- <sup>24</sup>D. McWilliams and D. W. Lynch, *Phys. Rev.* **130**, 2248 (1963).
- <sup>25</sup>T. N. Morgen, *Phys. Rev.* **139**, A343 (1965).
- <sup>26</sup>C. S. Hung and J. R. Gliessman, *Phys. Rev.* **96**, 1226 (1954).
- <sup>27</sup>E. M. Conwell, *Phys. Rev.* **103**, 51 (1956).
- <sup>28</sup>H. C. Casey, Jr., F. Ermanis, and K. B. Wolfstirn, *J. Appl. Phys.* **40**, 2945 (1969).
- <sup>29</sup>R. P. Khosla, *Phys. Rev.* **183**, 695 (1969).
- <sup>30</sup>W. A. Harrison, *Phys. Rev.* **104**, 1281 (1956).
- <sup>31</sup>J. Bardeen and W. Shockley, *Phys. Rev.* **80**, 72 (1950).
- <sup>32</sup>R. A. Smith, *Semiconductors* (Cambridge U.P., Cambridge, England, 1961), p. 147.
- <sup>33</sup>P. L. Chung, W. B. Whitten, and G. C. Danielson, *J. Phys. Chem. Solids* **26**, 1753 (1965).
- <sup>34</sup>E. Ehrenreich, *Phys. Rev.* **120**, 1951 (1960).
- <sup>35</sup>C. Kittel, *Introduction to Solid State Physics* (Wiley, New York, 1967), 3rd ed., p. 118.
- <sup>36</sup>W. Shockley, *Electrons and Holes in Semiconductors* (Van Nostrand, New York, 1950), p. 270.
- <sup>37</sup>F. J. Blatt, in *Solid State Physics*, Vol. 4, edited by F. Seitz and D. Turnbull (Academic, New York, 1957), p. 344.
- <sup>38</sup>C. Erginsoy, *Phys. Rev.* **79**, 1013 (1950).
- <sup>39</sup>L. R. Weisberg, *J. Appl. Phys.* **33**, 1817 (1962).
- <sup>40</sup>G. L. Pearson and H. Suhl, *Phys. Rev.* **83**, 768 (1951).
- <sup>41</sup>A. C. Beer, in Ref. 37, Suppl. 4, p. 44.
- <sup>42</sup>This equation is identical to Eq. (12) of Ref. 9 except for a change in sign of the coefficient of  $\cos 2\theta$  owing to the difference in our definition of the angle  $\theta$ .
- <sup>43</sup>C. Herring and E. Vogt, *Phys. Rev.* **101**, 944 (1955).
- <sup>44</sup>Reference 41, pp. 229–231.
- <sup>45</sup>A. H. Silson, *Theory of Metals* (Cambridge U. P., Cambridge, England, 1953), 2nd ed., p. 240.
- <sup>46</sup>R. S. Allgaier, *Phys. Rev.* **119**, 554 (1960).
- <sup>47</sup>C. Herring, *J. Appl. Phys.* **31**, 1939 (1960).
- <sup>48</sup>R. T. Bate, J. C. Bell, and A. C. Beer, *J. Appl. Phys.* **32**, 806 (1961).
- <sup>49</sup>C. Herring, *Bell System Tech. J.* **34**, 237 (1955), Appendix A.
- <sup>50</sup>R. A. Laff and H. Y. Fan, *Phys. Rev.* **112**, 317 (1958).
- <sup>51</sup>G. L. Pearson and C. Herring, *Physica* **20**, 975 (1954).
- <sup>52</sup>R. M. Broudy and J. D. Venables, *Phys. Rev.* **105**, 1757 (1957).
- <sup>53</sup>R. L. Weiher and B. G. Dick, Jr., *J. Appl. Phys.* **35**, 3511 (1964).
- <sup>54</sup>H. P. R. Frederikse, W. R. Hosler, and W. R. Thurber, *Phys. Rev.* **143**, 648 (1966).

## Optical and Electrical Properties of Cd<sub>2</sub>SnO<sub>4</sub>: A Defect Semiconductor

A. J. Nozik

*American Cyanamid Company, Central Research Division, Stamford, Connecticut 06904*  
(Received 10 February 1972)

Cd<sub>2</sub>SnO<sub>4</sub> has been found to be an *n*-type defect semiconductor in which oxygen vacancies provide the donor states. Crystalline powders and amorphous films with a wide range of conductivities have been prepared. Large Burstein shifts have been observed in the visible reflection and transmission spectra. Analysis of electrical and optical data on thin amorphous films of Cd<sub>2</sub>SnO<sub>4</sub> leads to a calculated optical band gap of 2.06 eV, a charge-carrier mobility of 10–20 cm<sup>2</sup>/V sec, and an effective mass 0.04 of the free-electron mass. The conductivity of amorphous films can be made as great as  $1.33 \times 10^3 \Omega^{-1} \text{cm}^{-1}$ , retaining high visible transmittance.

### I. INTRODUCTION

Cd<sub>2</sub>SnO<sub>4</sub> was first prepared by Smith,<sup>1</sup> who reported it to be bright yellow with an orthorhombic crystal structure. Others<sup>2,3</sup> have repeated the preparation, and improved x-ray powder-diffraction data have been published.<sup>4</sup> However, some unusual optical and electrical properties of Cd<sub>2</sub>SnO<sub>4</sub> have not been reported by the previous investiga-

tors. The present author has found that Cd<sub>2</sub>SnO<sub>4</sub> is an *n*-type defect semiconductor in which oxygen vacancies are believed to provide the donor states. The oxygen-vacancy concentration can be varied over a wide range, resulting in a correspondingly wide range of conductivities. A large Burstein shift<sup>5</sup> has also been observed in the optical spectra, which indicates a low free-carrier effective mass. Since large single crystals of Cd<sub>2</sub>SnO<sub>4</sub> were not

available, thin amorphous films of  $\text{Cd}_2\text{SnO}_4$  were prepared by sputtering and their electrical and optical properties measured. The band gap of these amorphous films has been derived from the optical data and the electron effective mass has been estimated from the Burstein shift. The electron mobility and conductivity of the amorphous films are unusually high. The relationship of these data to crystalline  $\text{Cd}_2\text{SnO}_4$  is discussed.

## II. EXPERIMENTAL

### A. Crystalline $\text{Cd}_2\text{SnO}_4$

Crystalline  $\text{Cd}_2\text{SnO}_4$  powder can be prepared by intimately mixing a 2:1 mole ratio of CdO and  $\text{SnO}_2$ , and heating the oxides at 1050 °C for 3–6 h. Alternatively, a stoichiometric mixed Cd-Sn hydrous oxide can be precipitated with base ( $\text{NH}_4\text{OH}$ , KOH, or NaOH) from an aqueous solution of the metal chlorides, the precipitate washed, dried, and calcined at temperatures from 900 to 1050 °C. The mixed hydrous oxide is a single-phase material which permits compound formation at lower reaction temperature.

The electrical conductivity of  $\text{Cd}_2\text{SnO}_4$  powder was measured by pressing pellets and attaching electrodes with silver-loaded epoxy. The sign of the charge carriers was determined from the polarity of the Seebeck voltage generated by the pressed pellets. Diffuse reflection spectra were obtained on lightly pressed 1-in. pellets; x-ray diffraction data were also obtained for powdered samples.

### B. Amorphous $\text{Cd}_2\text{SnO}_4$ Films

#### 1. Preparation

$\text{Cd}_2\text{SnO}_4$  films were prepared by rf sputtering from a polycrystalline  $\text{Cd}_2\text{SnO}_4$  target onto quartz or Pyrex substrates. The sputtering was carried out in a chamber in which the target was horizontally suspended over the substrate platform. The sputtering atmosphere was either pure argon or a mixture of argon and oxygen depending upon the desired conductivity of the  $\text{Cd}_2\text{SnO}_4$  films. Pressure was usually maintained at 10–20  $\mu$ . The substrate could be either water cooled or heated as high as 425 °C. A target-substrate distance of  $\sim 2\frac{1}{2}$  in. was used at a power level of 600 W. Under these conditions the deposition rate was  $\sim 0.5 \mu/\text{h}$ . Film stoichiometry was checked by determining the Cd/Sn ratio from x-ray emission data.

#### 2. Determination of Optical Constants

The refractive index was obtained by first measuring the film thickness using a multiple-beam interferometer. The transmission spectrum was then measured and the refractive index was calculated from

$$2nt = \lambda_1 \lambda_2 / (\lambda_1 - \lambda_2), \quad (1)$$

where  $n$  is the refractive index,  $t$  is the film thickness, and  $\lambda_1$  and  $\lambda_2$  are the wavelengths of two neighboring interference fringes (maxima or minima).

The complete expression for the transmission of a film supported on a substrate, including multiple reflection and interference effects, is complicated, and is given by Hall and Ferguson.<sup>6</sup> The values of  $\alpha$  in the region of the absorption edge were calculated from this expression using the known values of the refractive indices of  $\text{Cd}_2\text{SnO}_4$  and glass, and assuming  $n > k$  ( $= \lambda\alpha/4\pi$ ). In low-absorption regions where the interference effects are apparent,  $\alpha$  could simply be calculated at the transmission maxima from

$$\alpha = \frac{2}{t} \frac{n(n_g + 1)}{n^2 + n_g} \left[ \left( \frac{1}{T_m} \right)^{1/2} - 1 \right], \quad (2)$$

where  $n_g$  is the substrate refractive index and  $T_m$  is the transmittance of the sample (film on substrate vs substrate) at a wavelength corresponding to a transmission maximum.

### 3. Electrical Measurements

The conductivities of the films were measured using either a four-point probe resistivity rig or the voltage-probe method with painted Ag-epoxy electrodes. The Hall coefficients were measured simultaneously with the conductivity in the usual manner. A 12-kG electromagnet was used for this purpose. The sign of the charge carriers was determined from the Hall measurements and also from measurements with a thermoelectric hot probe.

## III. RESULTS

### A. Crystalline $\text{Cd}_2\text{SnO}_4$

When  $\text{Cd}_2\text{SnO}_4$  powder is prepared at temperatures above 900 °C, the orthorhombic phase reported by Smith<sup>1</sup> is formed. The conductivity and optical properties of this material were found to depend strongly upon the reaction environment and subsequent thermal history. If the synthesis was carried out in the presence of  $\text{O}_2$  and the reaction products cooled slowly ( $\sim 0.5$  °C/min), then  $\text{Cd}_2\text{SnO}_4$  was bright yellow with a room-temperature conductivity between  $10^{-1}$ – $10^{-3} \Omega^{-1} \text{cm}^{-1}$ . On the other hand, rapid quenching of the reaction product or synthesis in vacuum yielded green  $\text{Cd}_2\text{SnO}_4$  with a conductivity between  $1$ – $10 \Omega^{-1} \text{cm}^{-1}$ . Conductivity measurements at 77 and 300 °K indicated that this green material was degenerate. The sign of the charge carriers was  $n$  type for all samples.

The properties resulting from various preparative conditions for microcrystalline  $\text{Cd}_2\text{SnO}_4$  are summarized in Table I. Figure 1 shows diffuse reflection spectra of several powder samples. It is readily seen from Fig. 1 and Table I that the conductivity increase of  $\text{Cd}_2\text{SnO}_4$  is accompanied by

TABLE I. Effects of preparative conditions on the optical and electrical properties of crystalline  $\text{Cd}_2\text{SnO}_4$  powder.

Sample	Reaction atmosphere (1050°C, 6 h)	Cooling conditions	Color	Approximate absorption edge <sup>a</sup> (Å)	Powder conductivity ( $\Omega^{-1} \text{cm}^{-1}$ )
C, D	Vacuum	Quench in air	Green	4500	2-10
B	Air	Quench in air	Yellow	5150	0.5
	Air	16 h in air (uncontrolled)	Bright yellow	5250	0.05
	Air	20 h in air (0.5-5°C/min)	Bright yellow	5250	0.02
A	$\text{O}_2$	24 h in $\text{O}_2$ (0.2-1°C/min)	Bright yellow	5300	0.001

<sup>a</sup>Defined as wavelength where slope of diffuse reflection spectrum is a maximum.

a large shift of the fundamental optical-absorption edge toward the uv. This shift is the well-known Burstein effect.<sup>5</sup> The magnitude of the Burstein shift implies that the effective electron mass in  $\text{Cd}_2\text{SnO}_4$  is small.

For samples with high conductivities, the effects of free-carrier absorption become significant. As seen in Fig. 1, free-carrier absorption results in a decreased reflectance in the red for samples pre-

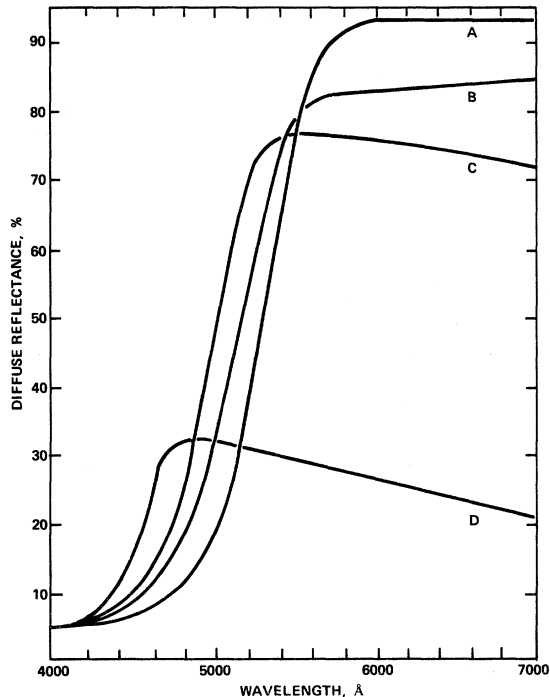


FIG. 1. Diffuse reflection spectra of  $\text{Cd}_2\text{SnO}_4$  powders prepared under various conditions. A: prepared and slow cooled in  $\text{O}_2$ ,  $\sigma \sim 0.01 \Omega^{-1} \text{cm}^{-1}$ ; B: prepared and quenched in air,  $\sigma \sim 0.5 \Omega^{-1} \text{cm}^{-1}$ ; C: prepared and quenched in vacuum,  $\sigma \sim 2.0 \Omega^{-1} \text{cm}^{-1}$ ; D: prepared and quenched in vacuum,  $\sigma \sim 6.0 \Omega^{-1} \text{cm}^{-1}$ .

pared in vacuum.

If  $\text{Cd}_2\text{SnO}_4$  is prepared at temperatures below 900°C, a new previously unreported crystalline phase appears. This phase has been tentatively identified from x-ray diffraction data as having a cubic spinel structure.<sup>7</sup>

#### B. Amorphous $\text{Cd}_2\text{SnO}_4$ Films

When the substrate is cooled during sputtering, the resultant films exhibit a single broad unstructured x-ray diffraction line. Such films are considered to be amorphous. If the x-ray pattern was due to small crystallite sizes, these would have to be under 25 Å to produce the observed line broadening. When the substrate is maintained at 425°C during sputtering, the films show a few broad x-ray lines which are unidentified, indicative, perhaps, of partial crystallization. If the amorphous films are heated to 700°C, crystallization of the cubic phase occurs. However, these films are reticulated and unsuitable for electrical and optical measurements. The partially crystallized films do not crystallize further with additional heating to 700°C. The x-ray emission data from the sputtered films showed a Cd/Sn ratio of 2:1 irrespective of the heat treatment and sputtering atmosphere.

The electrical and optical properties of the sputtered films can be controlled by varying the sputtering atmosphere and/or by heat treatment of the films after formation. Data were obtained on six films, and these are summarized in Table II. High conductivities were achieved by sputtering  $\text{Cd}_2\text{SnO}_4$  in pure Ar, or by heating films in  $\text{H}_2$  at (200-300)°C for 2-30 min. These films showed no change in their conductivities when cooled to 77°K, and hence were degenerate. Low conductivities were produced when the films were formed in the presence of  $\text{O}_2$  (50-75%). Sputtering conditions and subsequent thermal treatment were more important in determining the final film conductivity than the initial conductivity of the polycrystalline

TABLE II. Electrical and optical properties of Cd<sub>2</sub>SnO<sub>4</sub> films.<sup>a</sup>

Sample	Sputtering conditions <sup>b</sup> (atm, power, time)	Thickness ( $\mu$ )	Conductivity ( $\Omega^{-1} \text{ cm}^{-1}$ )	Sheet Resistance ( $\Omega/\text{sq}$ )	Hall coefficient ( $\text{cm}^3/\text{A sec}$ )	Mobility ( $\text{cm}^2/\text{V sec}$ )	Carrier density ( $\text{cm}^{-3}$ )	Apparent band gap (eV)
A	50% O <sub>2</sub> 700 W, 6 $\frac{1}{4}$ h	2.9	0.098	35 600	59.1	5.8	$1.1 \times 10^{17}$	2.06
B	20% O <sub>2</sub> , 600 W, 2 h	0.96	15.6	650	1.50	24	$4.3 \times 10^{18}$	2.28
C	100% Ar, 100 W, 1 h	0.23	100	430	0.10	10	$6.2 \times 10^{19}$	2.81
D	100% Ar, 200 W, 1 h	0.34	385	76	0.051	20	$1.2 \times 10^{20}$	2.85
E	50% O <sub>2</sub> 600 W, 6 $\frac{1}{2}$ h <sup>c</sup>	3.3	1330	2.3	...	...	...	2.51
F	20% O <sub>2</sub> , 700 W, 2 h, substrate at 425°C	1.0	82	1200	1.1	100	$5 \times 10^{18}$	...

<sup>a</sup>All data obtained at room temperature. All films are amorphous, except for film F which is partial crystallized.

<sup>b</sup>Substrate is water cooled except as noted. Sputtering atmosphere consists of Ar and O<sub>2</sub> as noted.

<sup>c</sup>Film was heated in H<sub>2</sub> at 280°C for 10 min.

Cd<sub>2</sub>SnO<sub>4</sub> target. The charge-carrier signs determined from the Hall measurements and the thermoelectric probe were in agreement, and always indicated *n*-type conduction.

Typical visible and near-infrared transmission spectra of low-conductivity and high-conductivity Cd<sub>2</sub>SnO<sub>4</sub> films are shown in Figs. 2 and 3. In these

figures, the film was initially sputtered in 50% O<sub>2</sub>, and then heat treated in H<sub>2</sub> at 280°C for 10 min. The large Burstein shift of the conductive film is clearly seen. The effects of free-carrier absorption in the conductive film are apparent in its reduced transmission in the red and near infrared. The oscillations in the spectra arise from inter-

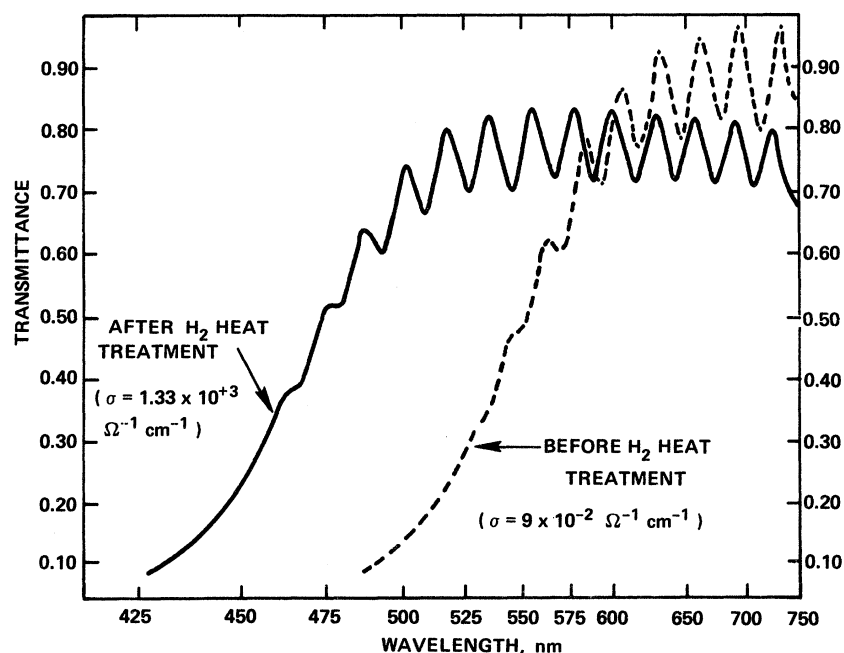


FIG. 2. Visible transmission spectra of Cd<sub>2</sub>SnO<sub>4</sub> thin films before and after H<sub>2</sub> heat treatment (film thickness 3.3  $\mu$ ).

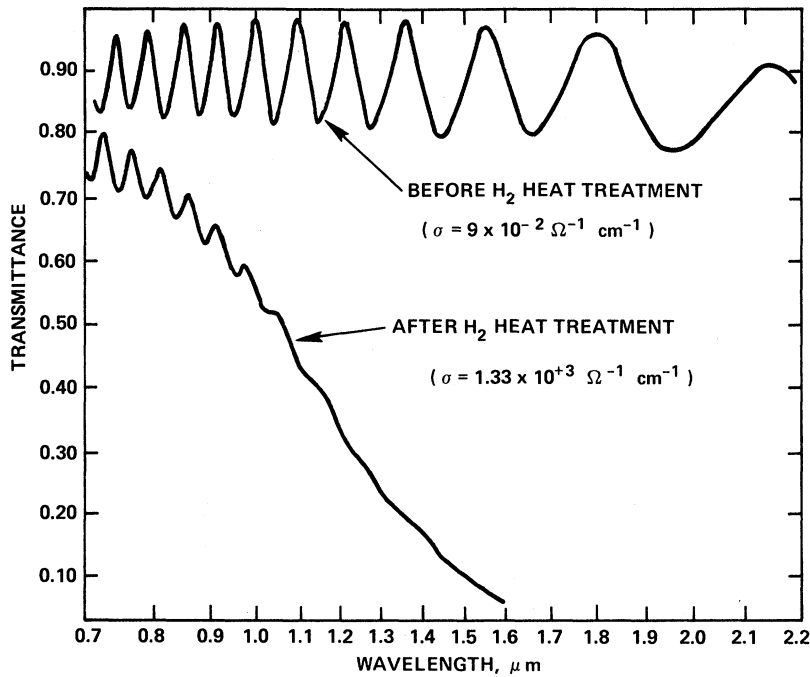


FIG. 3. Near infrared transmission spectra of  $\text{Cd}_2\text{SnO}_4$  thin films before and after  $\text{H}_2$  heat treatment (film thickness  $3.3 \mu$ ).

ference effects.

The dispersion curve for the refractive index of  $\text{Cd}_2\text{SnO}_4$  was determined for several films of high and low conductivity, and the results are plotted in Fig. 4. The shift of the dispersion edge toward the uv with increased conductivity is readily observed, and follows the corresponding shifts in the absorption edges.

The absorption coefficient  $\alpha$  was calculated from the transmission spectra, refractive index, and thickness of the films. The spectral dependence of  $\alpha$  for five films is plotted in Fig. 5. Again the large Burstein shifts in the conductive films are

readily seen, along with an attendant increase in free-carrier absorption. It is to be noted that the Burstein shift is apparently reversed in the most conductive film (film E). This effect is attributed to the influence of free-carrier absorption on the

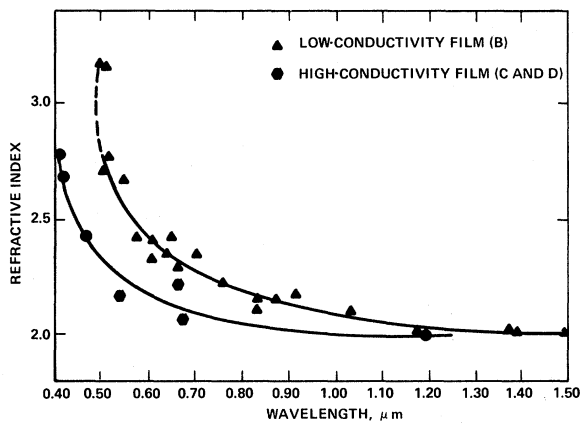


FIG. 4. Refractive index of  $\text{Cd}_2\text{SnO}_4$  for films with high and low conductivities. Film designations refer to Table II.

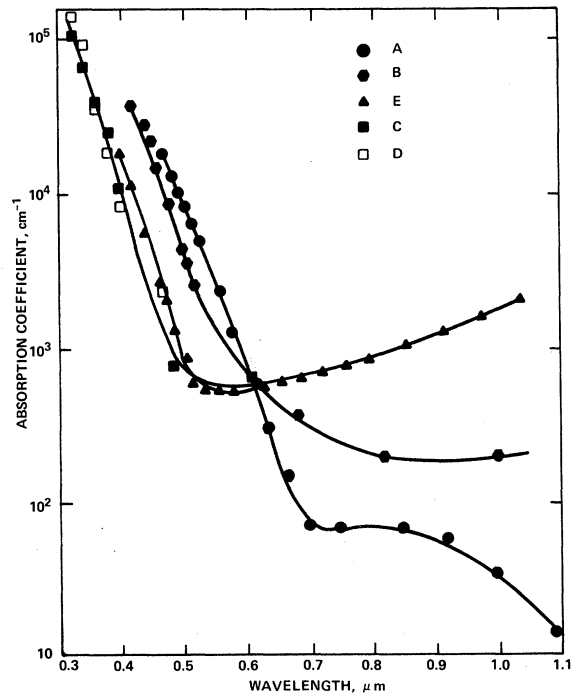


FIG. 5. Absorption coefficients of  $\text{Cd}_2\text{SnO}_4$  films. Film designations refer to Table II.

fundamental edge absorption. That is, at very high conductivities the free-carrier absorption in the visible is sufficient to significantly shift the apparent absorption edge toward the red.

An estimate of the optical band gap of  $\text{Cd}_2\text{SnO}_4$  can be derived from the absorption data. For most amorphous semiconductors, the energy dependence of  $\alpha$  in the absorbing region ( $\alpha \gtrsim 10^4 \text{ cm}^{-1}$ ) is given by<sup>8</sup>

$$\alpha = B(h\nu - E_0)^2/h\nu, \quad (3)$$

where  $B$  is a constant and  $E_0$  is the optical band gap. Hence, a plot of  $(\alpha h\nu)^{1/2}$  vs  $h\nu$  should be linear, and the intercept of the line on the abscissa at  $(\alpha h\nu)^{1/2} = 0$  yields the optical gap  $E_0$ . These data are plotted in Fig. 6 for five  $\text{Cd}_2\text{SnO}_4$  films. The plots are indeed linear, and the resultant values of  $E_0$  for each film sample are listed in Table II. The intrinsic optical gap of  $\text{Cd}_2\text{SnO}_4$  is 2.06 eV; the maximum optical gap induced by the Burstein shift in the conductive films is 2.85 eV.

#### IV. DISCUSSION

The conductivity of  $\text{Cd}_2\text{SnO}_4$  is attributed to the presence of oxygen vacancies which produce donor states in the forbidden gap. The large increase in conductivity and the onset of degeneracy in samples prepared in an oxygen deficient or reducing atmosphere is believed to be caused by an increase in the oxygen vacancy concentration ( $[\text{O}_v]$ ). Like-

wise, thermal quenching of  $\text{Cd}_2\text{SnO}_4$  freezes in the high-temperature  $[\text{O}_v]$  and this results in higher conductivities. The behavior of  $\text{Cd}_2\text{SnO}_4$  is analogous to that of other oxides, e. g.,<sup>9-12</sup> in which oxygen vacancies are known to exist. However, direct determination of the defect structure of  $\text{Cd}_2\text{SnO}_4$ , as, for example, via ESR studies, would be desirable.

It would also be desirable to measure the fundamental optical and transport properties of  $\text{Cd}_2\text{SnO}_4$  using large single crystals. However, crystals of sufficient size have not yet been prepared, and quantitative electro-optical data were therefore only obtained from amorphous thin films. In order to establish the significance of these data, the relationship between the behavior of amorphous and crystalline materials must be examined.

The value of 2.06 eV for the optical band gap of amorphous  $\text{Cd}_2\text{SnO}_4$  is believed to be a good estimate for the crystalline material as well. This is because the position of the optical-absorption edges of amorphous and crystalline forms are known to be similar.

The energy dependence of the absorption coefficient indicated in Eq. (3) is that expected for an indirect interband transition in crystalline semiconductors, wherein crystal momentum ( $\vec{k}$ ) is conserved by the emission or absorption of phonons. However, for amorphous materials, Eq. (3) is valid because the absence of translational symmetry allows a relaxation of the requirement for conservation of  $\vec{k}$ . Therefore, although the optical data for  $\text{Cd}_2\text{SnO}_4$  amorphous films fit Eq. (3) very well, one cannot conclude that crystalline  $\text{Cd}_2\text{SnO}_4$  is an indirect-band-gap semiconductor. Although a comparison of the diffuse reflection spectra of crystalline  $\text{Cd}_2\text{SnO}_4$  with that of the direct-gap semiconductor  $\text{CdS}$  would suggest that  $\text{Cd}_2\text{SnO}_4$  is an indirect material, data based on single crystals are required to settle this point.

The electronic mobilities and conductivities listed in Table II for  $\text{Cd}_2\text{SnO}_4$  amorphous films are relatively high, and represent the upper limit for currently known amorphous materials. As the mobility of amorphous materials is usually smaller than that of crystalline materials by at least 1-2 orders of magnitude, the mobility of crystalline  $\text{Cd}_2\text{SnO}_4$  would be expected to be much higher than the values listed in Table II. The partially crystallized film (film F) shows a mobility of  $100 \text{ cm}^2/\text{V sec}$ , which is consistent with this expectation.

An outstanding feature of the optical properties of  $\text{Cd}_2\text{SnO}_4$  is the large Burstein shift in conductive degenerate samples. This effect occurs in semiconductors with a low effective mass, and hence a conduction band with high curvature. The density of states at the bottom of the conduction band will be low in such a system. They can be saturat-

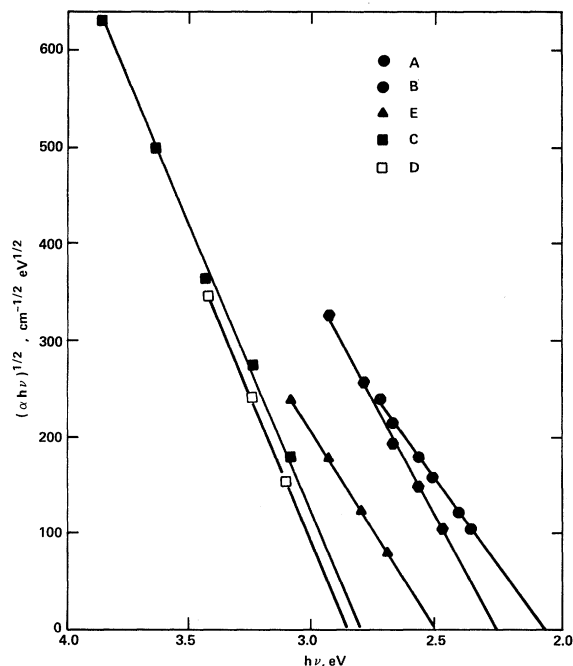


FIG. 6.  $(\alpha h\nu)^{1/2}$  vs  $h\nu$  for  $\text{Cd}_2\text{SnO}_4$  films. Film designations refer to Table II.

ed at relatively small free-carrier concentrations and force the fundamental optical absorption to proceed at higher energy. The observation of a Burstein shift in amorphous  $\text{Cd}_2\text{SnO}_4$  is apparently the first reported example of this effect in amorphous materials.

If it is assumed that the relationship between the effective mass and Burstein shift is equivalent for crystalline and amorphous semiconductors, then the effective mass of  $\text{Cd}_2\text{SnO}_4$  can be estimated from the band-edge shift and carrier densities listed in Table II. If one assumes spherical energy surfaces for the crystalline material, and that only the conduction band has high curvature, then<sup>13</sup>

$$N = (8\pi/3h^3)(2m^*\Delta E_g)^{3/2}, \quad (4)$$

where  $N$  is the free-carrier density,  $\Delta E_g$  is the Burstein shift, and  $m^*$  is the effective mass of the conduction electrons. At the lowest carrier density of  $4.3 \times 10^{18} \text{ cm}^{-3}$  the analysis yields

$$m^*/m_e \sim 0.04. \quad (5)$$

For  $\text{Cd}_2\text{SnO}_4$ , the effective mass increases with carrier density. This effect is observed for semiconductors with nonparabolic bands.<sup>14-16</sup> At carrier densities of  $6.2 \times 10^{19}$  and  $1.2 \times 10^{20} \text{ cm}^{-3}$ , the

effective-mass values are 0.08 and 0.11, respectively. These values are very low for a wide-band-gap oxide, and confirmation must be sought via other methods of measuring effective mass (i. e., infrared reflection and magnetoreflexion). For comparison, the effective masses at low carrier densities are 0.2 for CdS, 0.14 for CdO, and 0.4 for  $\text{SnO}_2$ .

Because of its large Burstein shift and relatively high mobility,  $\text{Cd}_2\text{SnO}_4$  becomes more transparent to visible light as its conductivity increases. This effect is moderated by the onset of significant free-carrier absorption at very high conductivities.  $\text{Cd}_2\text{SnO}_4$  films have a high ratio of conductivity to absorption coefficient, and since they are also tough, hard, and stable they have potential application as transparent electrodes. Furthermore, the relatively large band gap and small charge-carrier effective mass of  $\text{Cd}_2\text{SnO}_4$  make it potentially useful in various semiconductor devices.

#### ACKNOWLEDGMENTS

The author wishes to thank S. K. Deb for valuable suggestions and assistance, G. Haacke and F. E. Williams for helpful discussions, and L. A. Siegel for x-ray-diffraction data.

<sup>1</sup>A. J. Smith, *Acta Cryst.* **13**, 749 (1960).  
<sup>2</sup>M. Hassani, *J. Chem. (U. A. R.)* **9**, 275 (1966).  
<sup>3</sup>J. Choisnet, A. Deschanvres, and B. Raveau, *Compt. Rend.* **266c**, 543 (1968).  
<sup>4</sup>M. Trömel, *Naturwiss.* **54**, 17 (1967).  
<sup>5</sup>E. Burstein, *Phys. Rev.* **93**, 632 (1954).  
<sup>6</sup>J. F. Hall and W. F. C. Ferguson, *J. Opt. Soc. Am.* **45**, 714 (1955).  
<sup>7</sup>A. J. Nozik and L. A. Siegel (unpublished).  
<sup>8</sup>H. Fritzsche, *J. Non-Crystalline Solids* **6**, 49 (1971).  
<sup>9</sup>E. Mollwo and R. Stumpp, *Z. Physik* **184**, 286 (1965).

<sup>10</sup>M. Altwein, H. Finkenrath, C. Konák, J. Stuke, and G. Zimmerer, *Phys. Status Solidi* **29**, 203 (1968).  
<sup>11</sup>P. Höschl, C. Konák, and V. Prosser, *Mater. Res. Bull.* **4**, 87 (1969).  
<sup>12</sup>R. Haul, and D. Just, *J. Appl. Phys.* **33**, 487 (1962).  
<sup>13</sup>T. S. Moss, *Proc. Phys. Soc. (London)* **B67**, 775 (1954).  
<sup>14</sup>F. P. Koffyberg, *Can. J. Phys.* **49**, 435 (1971).  
<sup>15</sup>M. Cardona, *Phys. Rev.* **121**, 752 (1961).  
<sup>16</sup>G. B. Wright, A. J. Strauss, and T. C. Harman, *Phys. Rev.* **125**, 1534 (1962).